New Materials, Compounds and Applications
Vol.5, No.2, 2021, pp.122-131

Jomard Publishing

FABRICATION AND CHARACTERIZATION OF Au/MO/n-Si (MO: ZnO, In_2O_3, Al_2O_3) SCHOTTKY DIODES GROWN BY RF MAGNETRON SPUTTERING

Serkan Eymur, Nihat Tuğluoğlu*

Department of Energy Systems Engineering, Giresun University, Giresun, Turkey

Abstract. In this study, for investigating the effects of ZnO, In_2O_3 and Al_2O_3 interfacial layer, three types of Schottky diodes were fabricated by radio frequency (RF) magnetron sputtering method on the identical n-Si substrate with the same rectifier and ohmic contacts. The main diode parameters of them were determined from the current-voltage (*I-V*) characteristics at room temperature and compared in detail. The analysis of *I-V* plot showed a non-ideal diode behavior according to the thermionic emission technique due to the existence of interfacestates, interfacial layer, and series resistance. The measured values of *I-V* for all samples were utilized to compute the ideality factor (n), barrier height (Φ_b), series resistance (R_s) and interface state density (N_{ss}) values. The values of n and Φ_b of Au/ZnO/n-Si (**SD1**), Au/In_2O_3/n-Si (**SD2**) and Au/Al_2O_3/n-Si (**SD3**) Schottky diodes were calculated to be 2.05-0.707 eV, 2.19-0.675 eV and 1.23-0.773 eV, respectively. The lowest values of ideality factor, series resistance and density of interfacial states were obtained in Au/Al_2O_3/n-Si Schottky diode. These results show that the used the Al_2O_3 interlayer used in the Au/n-Si interface improves the performance of the metal-semiconductor diode rather than other metal oxides.

Keywords: *ZnO, In_2O_3, Al_2O_3, ideality factor, Barrier height, Schottky diode.*

Corresponding Author: *Nihat Tuğluoğlu, Department of Energy Systems Engineering, Giresun University, Giresun, Turkey, e-mail: tugluo@gmail.com*

Received: *24 June 2021;* ***Accepted:*** *31 July 2021;* ***Published:*** *07 August 2021.*

1. Introduction

The metal-semiconductor (MS) or metal-insulator-semiconductor (MIS) structures consist of semiconductor electronic devices, including solar cells, field effect transistors, light emitting detectors and integrated devices (Rhoderick *et al.*, 1988; Sze *et al.*, 2007). The analysis of electrical characteristics of the MIS type Schottky diodes at room temperature present not only full information about their conduction mechanism, but also provides to know the nature of barrier formation at the semiconductor-metal interface (Çiçek *et al.*, 2017; Nicollian *et al.*, 2002; Rhoderick *et al.*, 1988; Sze *et al.*, 2007). The reliability and performance of these MIS structures depend on series resistance, interface state density and the creation of the insulator layer between semiconductor-metal interface. If the oxide layer at the interface between the metal and the semiconductor is a few nanometers thick, it transforms the structure into a metal-insulator-semiconductor (MIS) structure. Ultimately, this oxide layer can modify the barrier height of the MIS structure (Altındal *et al.*, 2003; Altındal *et al.*, 2019; Karadeniz *et al.*, 2004). Interfacial oxide layer and an interface states at metal–semiconductor (MS) contact plays a major act in the estimation of the barrier height.

Transparent conducting oxides (TCOs) such as zinc oxide (ZnO) and indium oxide (In_2O_3) comprise a special category of materials having huge expects due to

their high transparency in the visible region of the spectrum and unique semiconducting properties along with very low resistivity (10^{-3} Ω·cm to 10^{-4} Ω·cm). A wide range of applications of TCOs contains their utilize as transparent electrodes in the photovoltaics (Yu *et al.*, 2016), gas sensing devices (Ram, 2013), functional (protective, decorative) coatings (Sotelo-Vazquez *et al.*, 2015) and organic light emitting diodes (Afshinmanesh *et al.*, 2014). ZnO thin films have low absorption coefficient in the visible region, valued refractive index, wide band gap at ~ 3.36 eV and high exciton binding energy at 60 MeV (Meriche *et al.*, 2015; Tiwari *et al.*, 2015). In_2O_3 thin films are characterized by notable physical properties such as low electrical resistivity (10^{-1} -10^{-3} Ω.cm), high optical transparency (60–85%) and wide direct band gap energy (3.4–3.8 eV) (Souli *et al.*, 2021). ZnO and In_2O_3 thin films are utilized with many applications in different domains such as solar cells (Erfurt *et al.*, 2020; Khadtare *et al.*, 2017), gas sensing (E. Cao *et al.*, 2020; Hjiri *et al.*, 2014) and optoelectronics (Narmada *et al.*, 2020; Kim *et al.*, 2006).

Al_2O_3 thin films have received much attention for their perfect electrical, optical, thermal, chemical and mechanical properties. Al_2O_3 thin films are used in several areas such as optics, microelectronics, and optoelectronics (Balakrishnan *et al.*, 2010; Sridharan *et al.*, 2007; Tang *et al.*, 2012). ZnO, In_2O_3 and Al_2O_3 thin films can be deposited using several techniques including sputtering, atomic layer deposition (ALD), pulsed laser deposition (PLD), chemical vapor deposition (CVD) and the sol-gel method (Narmada *et al*., 2020; L. Cao *et al.*, 2011; Keskenler *et al.*, 2013; Khan *et al.*, 2012; Koh *et al.*, 1997; Suárez-García *et al.*, 2003). Among different methods of metal oxide thin films growth reported in literature, it is known that the RF magnetron sputtering is a technique of choice for device development. As a result, in this study the RF magnetron sputtering was chosen due to the aptitude of a no toxic gas emission, good uniformity, high deposition rate, quite good adherence and high composition control (Hu *et al.*, 2017; Shi *et al.*, 2013; Sundaram *et al.*, 1997; Yang *et al.*, 2009).

It is observed that many researchers have focused on ZnO, In_2O_3 and Al_2O_3 metal oxide thin films-based device in literature (Gullu *et al.*, 2019; Gupta *et al.*, 2013; Özmen *et al.*, 2019). Unfortunately, there is not enough work on the electrical characterization of Schottky diodes with metal oxide film fabricated with rf sputtering.In the present work, a systematic study of Schottky diodes with different metal oxide thin film has been carried out using radio frequency (RF) magnetron sputtering.The characteristic diode parameters of the produced diodes were calculated using the current-voltage technique and compared with each other. Consequently, we reported the diode parameters such as ideality factor, barrier height, series resistance and interface state density of the prepared diodes. The diodes were characterized by current–voltage (*I-V*) measurements to better understand the effect of the produced metal oxides.

2. Experimental

For electrical measurements the studied metal oxide structures were created on the phosphorus doped n-Si (100) wafers with 380 μm thick and 20 Ω-cm resistivity.n-Si substrate with 2 inch diameter was chemically cleaned using the RCA cleaning method to eliminate the native oxide layer and impurities. Gold (Au) (with a purity 99.99% and thickness of 200 nm) was thermally evaporated to the entire back surface of the Si layer by a vacuum evaporation system and later annealed at 500°C for 5 min in nitrogen

atmosphere to create Au ohmic contact.Si substrate was cut into 4 equal parts and 3 quarters were used. Each of the parts was used to deposit ZnO, In_2O_3 and Al_2O_3 thin films. The ZnO (99.999% purity), In_2O_3 (99.99% purity) and Al_2O_3 (99.99% purity) sputter target materials with 2 inch diameter were used in this work. The ZnO, In_2O_3 and Al_2O_3 thin films were deposited on the non-ohmic contact surface of n-Si substrate by radio frequency (RF) magnetic sputtering method. Then, circular gold (Au) rectifier contacts with a radius of 2 mm and thickness of 200 nm on ZnO, In_2O_3 and Al_2O_3 thin films were prepared with a thermal evaporation system.As a result, Au/ZnO/n-Si/Au, Au/In_2O_3/n-Si/Au and Au/Al_2O_3/n-Si/Au Schottky diodes were fabricated.During the thin film deposition, the distance between the substrate and the target was 15 cm.The studying gas for sputtering the films was argon (Ar, 99.999%, high purity), with a flow ratio of 30% O_2 (99.999%) added into Ar as the reaction gas.The working pressure was set to 1.2 Pa while the base pressure inside the chamber was kept at 1 $\times 10^{-3}$ Pa. n-Si wafer was rotated at a speed of 20 rpm to increase the uniformity in thin film growing. The power of sputtering for all films was set to 100 W. The deposition ratio of the films was about 5 nm/min. 50 nm thick film was grown for all the films. The prepared Schottky diodes were characterized by current-voltage (I-V) measurements. The I-V values for the diodes were collected using Keithley 2400 Sourcemeter in the voltage range from +1 V to -1 V at room temperature.

3. Results and Discussion

The main electrical properties of the fabricated Au/MO/n-Si (MO: ZnO (SD1), In_2O_3(SD2), Al_2O_3(SD3)) Schottky diodes were determined by using the reverse and forward bias I-V measurements of the diodes under dark conditions. It can be seen from Fig. 1 that all SD1, SD2 and SD3 diodes show a good rectification behavior. The rectification ratio values of the SD1, SD2 and SD3 diodes (measured for ± 1 V) were calculated as 32663, 1316 and 44, respectively.According to thermionic emission theory (TE), the forward bias current of a diode can be written as (Rhoderick *et al.*, 1988; Sze *et al.*, 2007; Yalcin *et al.*, 2020; Yuksel *et al.*, 2013):

$$I = I_0\left[exp\left(\frac{q(V-IR_s)}{nkT}\right)-1\right] \quad (1)$$

where V is the applied voltage, T is the ambient temperature in Kelvin, n is the ideality factor, R_s is the series resistance, q and k are defined as the electronic charge and the Boltzmann constant, respectively. I_0 is defined as the saturation current and can be given as:

$$I_0 = AA^*T^2 exp\left[-\frac{q\Phi_B}{kT}\right] \quad (2)$$

where A, A* and Φ_B are the diode area, the effective Richardson coefficient for n-Si and the barrier height, respectively.

$$\Phi_B = \frac{kT}{q} ln\left(\frac{AA^*T^2}{I_0}\right) \quad (3)$$

$$n = \frac{q}{kT}\frac{dV}{d(lnI)} \quad (4)$$

The values of n for the samples were found from the slope of the linear region of the I-V plot and illustrated in Table 1. The lowest n value was obtained as 1.23 for Al_2O_3/n-Si (SD3) Schottky diode. When Fig. 1 and Table 1 are examined, the ideality factor value deviated from equation 1 according to the TE theory for all samples. The reason of this can be attributed to tunneling current flow due to the interfacial layer and a diversity of dominating effect of conduction mechanism depending on recombination-generation current in the junction region (Schroder, 2006; Chin *et al*., 1993; Olikh, 2015). The values of Φ_B for the samples were calculated from the intercept of the linear region of the I–V plot and illustrated in Table 1. The largest Φ_B value was determined as 0.773 for Al_2O_3/n-Si (SD3) Schottky diode.

Table 1. The basic electrical parameters determined from I-V measurements of the studied Schottky structures

Sample	I_o (A)	n	Φ_B (eV)
ZnO/n-Si	4.38×10^{-7}	2.05	0.707
In_2O_3/n-Si	1.48×10^{-6}	2.19	0.675
Al_2O_3/n-Si	3.30×10^{-8}	1.23	0.773

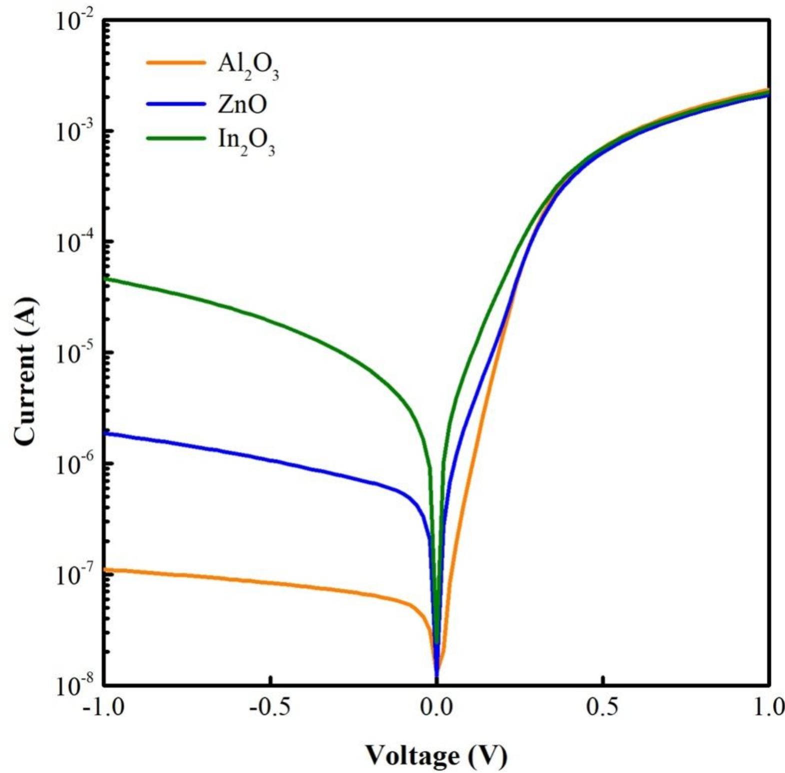

Fig. 1. Variation of the current (I) with voltage (V) for all the samples

The series resistance (R_s) is a significant parameter for the I-V characteristics of the studied Schottky structures. The downward-bending curve of the IV plot at high voltages show the influence of R_s (Altındal *et al*., 2010). Therefore, in the high current region, Φ_B, n and R_s were estimated by a technique that was introduced by Cheung and

Cheung functions (Cheung *et al*., 1986). According to Eq. (1), the following Cheung and Cheung equations can be given as

$$\frac{dV}{d\ln(I)} = \frac{nkT}{q} + IR_s \tag{5}$$

$$H(I) = V - \left(\frac{nkT}{q}\right)\ln\left(\frac{I}{AA^*T^2}\right) = n\Phi_B + IR_s \tag{6}$$

Fig. 2 and 3 present the linear dependence of $dV/d(\ln(I))$ and $H(I)$ vs. I according to equations (5) and (6), respectively. The slope and intercept of the solid line shown in curve of $dV/d(ln(I))$ and $H(I)$ vs. I allowed calculation of the R_S and n values for the all samples, respectively. These calculated values were presented in Table 2. In addition, plot of $H(I)$ vs. I yields a Φ_B and R_S values of the studied Schottky diodes. These calculated values were presented in Table 2. It is observed that the values of R_s determined by Eqs. (5) and (6) are in good agreement with each other. It is seen from Table 2 that the R_s and n values of the Al_2O_3/n-Si (SD3) Schottky diode obtained from $dV/d(ln(I))$vs. I are found to be 294 Ω and 1.03 and the Φ_B and R_s values from $H(I)$ vs. I curve are 0.812 eV and 270Ω, respectively at room temperature.

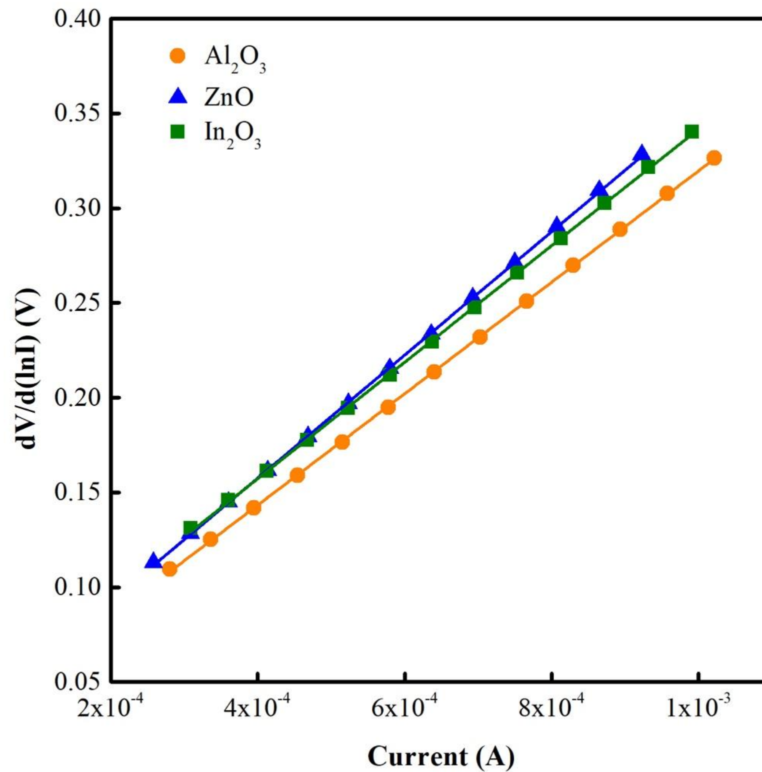

Fig. 2. The dV/d ln(I) versus I plots ofthe studied Schottky diode structures

Table 2. Main electrical parameters of the studied Schottky structures obtained from Cheung functions

Sample	d*V*/d ln(*I*) -*I*		H(*I*)-*I*	
	R_s (Ω)	n	R_s (Ω)	Φ_B (eV)
ZnO/n-Si	325	1.10	307	0.795
In_2O_3/n-Si	307	1.37	290	0.733
Al_2O_3/n-Si	294	1.03	270	0.812

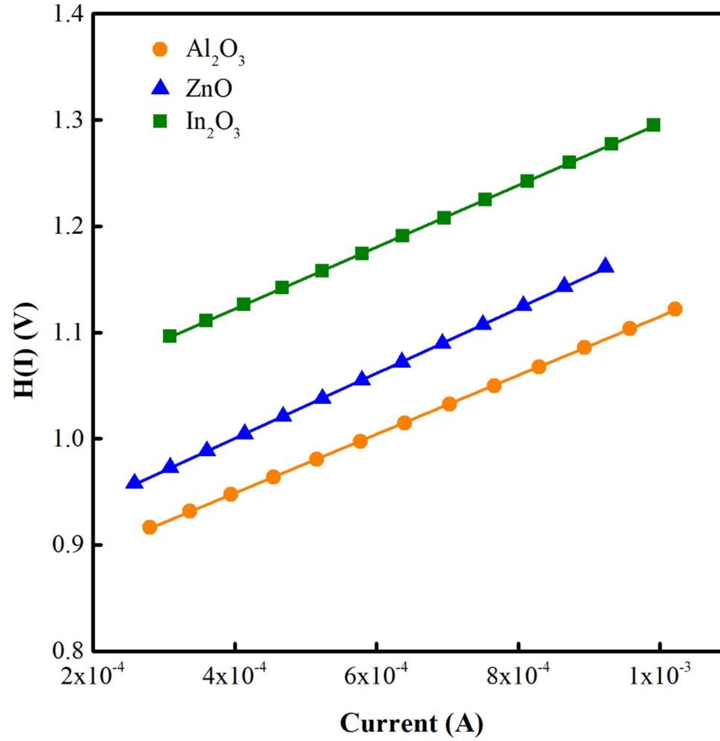

Fig. 3. The H(*I*) versus *I* plots ofthe studied Schottky diode structures

The energy profile of the interface states ($E_c - E_{ss}$), the density of interface states (N_{ss}) and the effective barrier height (Φ_e) values for the studied Schottky diodes can be estimated from the following equations (Sze, 1981; Rhoderick *et al*., 1988):

$$\Phi_e = \Phi_b + \beta V = \Phi_b + \left(1 - \frac{1}{n(V)}\right)V \tag{7}$$

$$N_{ss} = \frac{1}{q}\left(\frac{\varepsilon_i}{\delta}\left(n(V) - 1\right) - \frac{\varepsilon_s}{W_D}\right) \tag{8}$$

$$E_c - E_{ss} = q\left(\Phi_e - V\right) \tag{9}$$

where δ is the interfacial layer thickness ($\delta \cong$ 50 nm for the samples), E_c is the conduction band edge, E_{ss} is the energy of the interface states, $\varepsilon_s = 11.8\varepsilon_0$ and $\varepsilon_i = 8.5, 8.9$ and $9.86\varepsilon_0$ for ZnO, In_2O_3 and Al_2O_3, respectively) are silicon semiconductor and the permittivity of interfacial layers, respectively.

The values of N_{ss} found as a function of voltage are converted to a function of $(E_c - E_{ss})$ according to Eq. 9. The density of interface state versus energy distribution plot of the device at room temperature is given in Fig. 4. As observed, in the range from $E_c - 0.46$ to $E_c - 0.65$ eV, the N_{ss} values were found to change from 8.20 x 10^{12} $eV^{-1}cm^{-2}$ to 1.16 x 10^{12} $eV^{-1}cm^{-2}$, respectively for Al_2O_3/n-Si Schottky diode. It is evidently seen from Fig. 4 that the values of N_{ss} increase with decreasing energy and the exponential growth of the interface state density from midgap towards to the bottom of the conduction band of the n-Si. The lowest N_{ss} value was determined for Al_2O_3/n-Si (SD3) Schottky diode.

As a result, in the light of the above information, diode parameter values such as Φ_B, n, R_s and N_{ss} were determined with different techniques for all samples prepared. The diode parameter values obtained for the Al_2O_3/n-Si Schottky diode gave the best results among the diodes produced under the same conditions and with the same interfacial layer thicknesses.As one of the reasons for this result, it can be said that the dielectric constant of Al_2O_3 is higher than the others and it has a low leakage current.

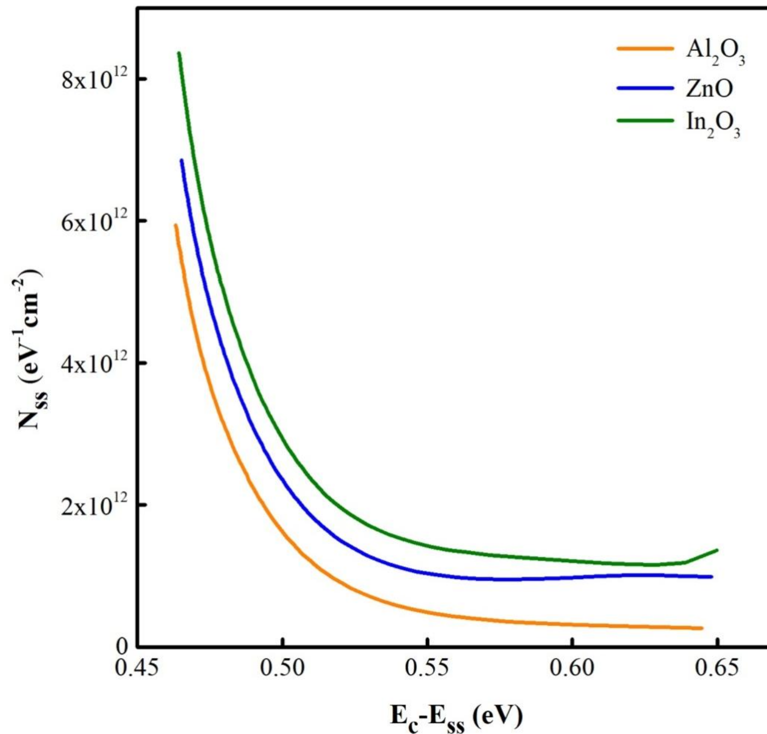

Fig. 4. The energy distribution profile of the N_{ss} determined from the forward *I-V* characteristics for the samples

4. Conclusion

In this work, we have fabricated Au/Al_2O_3/n-Si/Au, Au/ZnO/n-Si/Au and Au/In_2O_3/n-Si/Au Schottky diodes. The electrical properties of Al_2O_3, In_2O_3 and ZnO films deposited by rf magnetron sputtering on n-Si substrate were investigated and discussed. The metal oxide layers on the n-Si indicated a good rectifying behavior. The

sputtering deposited metal oxide films were the thickness of 50 nm. For this purpose, *I-V* measurements were taken in dark and at room temperature and ideality factor (*n*) values for Al_2O_3, ZnO and In_2O_3/n-Si contact found to be 1.23, 2.05 and 2.19, respectively. Furthermore, barrier height values for Al_2O_3, ZnO and In_2O_3/n-Si contact found to be 0.773 eV, 0.707 eV and 0.675 eV, respectively. The ideality factor value of 1.23 for Al_2O_3/n-Si diode is lower while the barrier height value of 0.773 eV for the same diode is larger than the values reported for ZnO/n-Si or In_2O_3/n-Si diodes. It was obtained that the values of *n* computed from I-V measurement were larger than unity. The deviation from the ideal behavior is explained on the basis of interface state density and series resistance. The series resistance parameter of these diodes was extracted from the Cheung functions and computed as 294 Ω, 307 Ω and 325 Ω for Al_2O_3, In_2O_3 and ZnO thin film, respectively. As a result, metal oxide thin film interface layer deposited with rf magnetron sputtering on n-Si can be utilized as an alternative to other methods and for obtaining diodes with higher barrier height.

Acknowledgment

This study was supported by The ManagementUnit of Scientific Research Project of Giresun University under Project No. FEN-BAP-A-270220-43.

References

Afshinmanesh, F., Curto, A.G., Milaninia, K.M., van Hulst, N.F., & Brongersma, M.L. (2014). Transparent Metallic Fractal Electrodes for Semiconductor Devices. *Nano Letters, 14*(9), 5068-5074.

Altındal, Ş., Karadeniz, S., Tuğluoğlu, N., & Tataroğlu, A. (2003). The role of interface states and series resistance on the I–V and C–V characteristics in Al/SnO2/p-Si Schottky diodes. *Solid-State Electronics, 47*(10), 1847-1854.

Altındal, Ş., Şafak, Y., Taşçıoğlu, İ., Özbay, E. (2010). The effect of insulator layer thickness on the main electrical parameters in (Ni/Au)/AlxGa1−xN/AlN/GaN heterostructures. *Surface and Interface Analysis, 42(6-7)*, 803-806.

Altındal, Ş., Sevgili, Ö., & Azizian-Kalandaragh, Y. (2019). A comparison of electrical parameters of Au/n-Si and Au/(CoSO4–PVP)/n-Si structures (SBDs) to determine the effect of (CoSO4–PVP) organic interlayer at room temperature. *Journal of Materials Science: Materials in Electronics, 30*(10), 9273-9280.

Balakrishnan, G., Kuppusami, P., Sundari, S. T., Thirumurugesan, R., Ganesan, V., Mohandas, E., & Sastikumar, D. (2010). Structural and optical properties of γ-alumina thin films prepared by pulsed laser deposition. *Thin Solid Films, 518*(14), 3898-3902.

Cao, E., Song, G., Guo, Z., Zhang, Y., Hao, W., Sun, L., & Nie, Z. (2020). Acetone sensing characteristics of Fe2O3/In2O3 nanocomposite. *Materials Letters, 261*, 126985. doi:https://doi.org/10.1016/j.matlet.2019.126985

Cao, L., Zhu, L., Jiang, J., Zhao, R., Ye, Z., & Zhao, B. (2011). Highly transparent and conducting fluorine-doped ZnO thin films prepared by pulsed laser deposition. *Solar Energy Materials and Solar Cells, 95*(3), 894-898. doi:https://doi.org/10.1016/j.solmat.2010.11.012

Cheung, S.K., Cheung, N.W. (1986). Extraction of Schottky diode parameters from forward current- voltage characteristics. *Applied Physics Letters*, *49*(2), 85-87.

Chin, V.W.L., Green, M.A., Storey, J.W.V. (1993). Current transport mechanisms studied by I-V-T and IR photoemission measurements on a P-doped PtSi Schottky diode. *Solid State Electronics*, *36*(8), 1107-1116.

Çiçek, O., Uslu Tecimer, H., Tan, S. O., Tecimer, H., Orak, İ., & Altındal, Ş. (2017). Synthesis and characterization of pure and graphene (Gr)-doped organic/polymer nanocomposites to investigate the electrical and photoconductivity properties of Au/n-GaAs structures. *Composites Part B: Engineering, 113*, 14-23. doi:https://doi.org/10.1016/j.compositesb.2017.01.012

Erfurt, D., Koida, T., Heinemann, M. D., Li, C., Bertram, T., Nishinaga, J., . . . Schlatmann, R. (2020). Impact of rough substrates on hydrogen-doped indium oxides for the application in CIGS devices. *Solar Energy Materials and Solar Cells, 206*, 110300. doi:https://doi.org/10.1016/j.solmat.2019.110300

Gullu, H.H., & Yildiz, D.E. (2019). Analysis of forward and reverse biased current–voltage characteristics of Al/Al2O3/n-Si Schottky diode with atomic layer deposited Al2O3 thin film interlayer. *Journal of Materials Science: Materials in Electronics, 30*(21), 19383-19393. doi:10.1007/s10854-019-02300-1

Gupta, R.K., & Yakuphanoglu, F. (2013). Analysis of device parameters of Al/In2O3/p-Si Schottky diode. *Microelectronic Engineering, 105*, 13-17. doi:https://doi.org/10.1016/j.mee.2012.12.026

Hjiri, M., El Mir, L., Leonardi, S.G., Pistone, A., Mavilia, L., & Neri, G. (2014). Al-doped ZnO for highly sensitive CO gas sensors. *Sensors and Actuators B: Chemical, 196*, 413-420. doi:https://doi.org/10.1016/j.snb.2014.01.068

Hu, Y. M., Li, J.Y., Chen, N.Y., Chen, C.Y., Han, T.C., & Yu, C.C. (2017). Effect of sputtering power on crystallinity, intrinsic defects, and optical and electrical properties of Al-doped ZnO transparent conducting thin films for optoelectronic devices. *Journal of Applied Physics, 121*(8), 085302. doi:10.1063/1.4977104

Karadeniz, S., Tuğluoğlu, N., & Serin, T. (2004). Substrate temperature dependence of series resistance in Al/SnO2/p-Si (111) Schottky diodes prepared by spray deposition method. *Applied Surface Science, 233*(1), 5-13. doi:https://doi.org/10.1016/j.apsusc.2004.03.216

Keskenler, E.F., Tomakin, M., Doğan, S., Turgut, G., Aydın, S., Duman, S., & Gürbulak, B. (2013). Growth and characterization of Ag/n-ZnO/p-Si/Al heterojunction diode by sol–gel spin technique. *Journal of Alloys and Compounds, 550*, 129-132. doi:https://doi.org/10.1016/j.jallcom.2012.09.131

Khadtare, S., Bansode, A.S., Mathe, V.L., Shrestha, N.K., Bathula, C., Han, S.-H., & Pathan, H.M. (2017). Effect of oxygen plasma treatment on performance of ZnO based dye sensitized solar cells. *Journal of Alloys and Compounds, 724*, 348-352. doi:https://doi.org/10.1016/j.jallcom.2017.07.013

Khan, M.A.M., Khan, W., Ahamed, M., & Alhoshan, M. (2012). Structural and optical properties of In2O3 nanostructured thin film. *Materials Letters, 79*, 119-121. doi:https://doi.org/10.1016/j.matlet.2012.03.110

Kim, T. W., Choo, D. C., No, Y. S., Choi, W. K., & Choi, E. H. (2006). High work function of Al-doped zinc-oxide thin films as transparent conductive anodes in organic light-emitting devices. *Applied Surface Science, 253*(4), 1917-1920. doi:https://doi.org/10.1016/j.apsusc.2006.03.032

Koh, W., Ku, S.-J., & Kim, Y. (1997). Chemical vapor deposition of Al2O3 films using highly volatile single sources. *Thin Solid Films, 304*(1), 222-224. doi:https://doi.org/10.1016/S0040-6090(97)00132-6

Meriche, F., Touam, T., Chelouche, A., Dehimi, M., Solard, J., Fischer, A.,Peng, L.-H. (2015). Post-annealing effects on the physical and optical waveguiding properties of RF sputtered ZnO thin films. *Electronic Materials Letters, 11*(5), 862-870. doi:10.1007/s13391-015-5005-1.

Narmada, A., Kathirvel, P., Mohan, L., Saravanakumar, S., Marnadu, R., & Chandrasekaran, J. (2020). Jet nebuliser spray pyrolysed indium oxide and nickel doped indium oxide thin films for photodiode application. *Optik*, *202*, 163701.

Nicollian, E. H., & Brews, J. R. (2002). *MOS (Metal Oxide Semiconductor) Physics and Technology*: Wiley.

Olikh,O.Y. (2015) Review and test of methods for determination of the Schottky diode parameters. *Journal of Applied Physics*, 118, 024502.

Özmen, A., Aydogan, S., & Yilmaz, M. (2019). Fabrication of spray derived nanostructured n-ZnO/p-Si heterojunction diode and investigation of its response to dark and light. *Ceramics International, 45*(12), 14794-14805.

Ram, S. (2013). Metal Oxide Nanostructures as Gas Sensing Devices, G. Eranna. *Materials and Manufacturing Processes, 28*(11), 1277-1278. doi:10.1080/10426914.2012.736667

Rhoderick, E.H.,Williams, R.H. (1988). *Metal-Semiconductor Contacts*. Oxford Clarendon Press.

Schroder, D.K. (2006) *Semiconductor Material and Device Characterization*. Wiley, New York.

Shi, Q., Zhou, K., Dai, M., Hou, H., Lin, S., Wei, C., & Hu, F. (2013). Room temperature preparation of high performance AZO films by MF sputtering. *Ceramics International, 39*(2), 1135-1141. doi:https://doi.org/10.1016/j.ceramint.2012.07.037

Sotelo-Vazquez, C., Noor, N., Kafizas, A., Quesada-Cabrera, R., Scanlon, D.O., Taylor, A., Parkin, I. P. (2015). Multifunctional P-Doped TiO2 Films: A New Approach to Self-Cleaning, Transparent Conducting Oxide Materials. *Chemistry of Materials, 27*(9), 3234-3242. doi:10.1021/cm504734a

Souli, M., Ajili, L., Alhalaili, B., Khadaraoui, A., Vidu, R., & Kamoun-Turki, N. (2021). Enhancement in structural, optical and morphological properties of sprayed In2O3 thin films induced by low energy electron beam irradiation. *Materials Science in Semiconductor Processing, 124*, 105595.

Sridharan, M., Sillassen, M., Bøttiger, J., Chevallier, J., & Birkedal, H. (2007). Pulsed DC magnetron sputtered Al2O3 films and their hardness. *Surface and Coatings Technology, 202*(4), 920-924. doi:https://doi.org/10.1016/j.surfcoat.2007.05.061

Suárez-García, A., Gonzalo, J., & Afonso, C. N. (2003). Low-loss Al2O3 waveguides produced by pulsed laser deposition at room temperature. *Applied Physics A, 77*(6), 779-783. doi:10.1007/s00339-003-2212-7

Sundaram, K.B., & Khan, A. (1997). Characterization and optimization of zinc oxide films by r.f. magnetron sputtering. *Thin Solid Films, 295*(1), 87-91.

Sze, S.M. (1981). *Physics of Semiconductor Devices*. Hoboken, N.J.: Wiley-Interscience.

Sze, S.M., & Ng, K.K. (2007). *Physics of Semiconductor Devices*. Hoboken, N.J.: Wiley-Interscience.

Tang, X., Luo, F., Ou, F., Zhou, W., Zhu, D., & Huang, Z. (2012). Effects of negative substrate bias voltage on the structure and properties of aluminum oxide films prepared by DC reactive magnetron sputtering. *Applied Surface Science, 259*, 448-453. doi:https://doi.org/10.1016/j.apsusc.2012.07.064

Tiwari, N., Shieh, H.-P. D., & Liu, P.-T. (2015). Structural, optical, and photoluminescence study of ZnO/IGZO thin film for thin film transistor application. *Materials Letters, 151*, 53-56. doi:https://doi.org/10.1016/j.matlet.2015.03.043

Yalcin, M., Ozmen, D., & Yakuphanoglu, F. (2020). Sr-doped yttrium nickel oxide-based photodetectors. *Journal of Materials Science - Materials in Electronics, 31*(4), 3441-3455. doi:https://doi.org/10.1007/s10854-020-02892-z

Yang, W., Liu, Z., Peng, D.-L., Zhang, F., Huang, H., Xie, Y., & Wu, Z. (2009). Room-temperature deposition of transparent conducting Al-doped ZnO films by RF magnetron sputtering method. *Applied Surface Science, 255*(11), 5669-5673.

Yu, X., Marks, T. J., & Facchetti, A. (2016). Metal oxides for optoelectronic applications. *Nature Materials, 15*(4), 383-396.

Yuksel, O.F., Tugluoglu, N., Safak, H., Nalcacigil, Z., Kus, M., & Karadeniz, S. (2013). Analysis of temperature dependent electrical properties of Au/perylene-diimide/n-Si Schottky diodes. *Thin Solid Films, 534*, 614-620.